

Cation Vibrational Spectra of Indole and Indole–Argon van der Waals Complex. A Zero Kinetic Energy Photoelectron Study

Tomáš Vondrák, Shin-ichiro Sato, and Katsumi Kimura*

School of Materials Science, Japan Advanced Institute of Science and Technology, Tatsunokuchi, Ishikawa 923-12, Japan

Received: September 11, 1996; In Final Form: January 23, 1997[⊗]

Zero kinetic energy (ZEKE) photoelectron spectra of indole obtained via nine vibrational levels of the $S_1(^1L_b)$ manifold (namely, 0^0 , 42^2 , 41^2 , 29^1 , $39^1 42^1$, 28^1 , 27^1 , 26^1 , and 37^2) are reported. The adiabatic ionization energy of indole has been determined to be $I_a = 62592 \pm 4 \text{ cm}^{-1}$ ($7.7604 \pm 0.0005 \text{ eV}$). Cation fundamental vibrational modes up to 807 cm^{-1} above the D_0 origin have been determined on the basis of the $\Delta\nu = 0$ propensity. The presence of the $\Delta\nu = 1$ excitation for the out-of-plane modes indicates the presence of a significant vibronic interaction in the ground state cation. For the van der Waals (vdW) complex of indole with Ar, it has been found that the red shift in the S_1 origin amounts to 27 cm^{-1} upon the complex formation, whereas the decrease in I_a is 88 cm^{-1} with respect to indole. The ZEKE D_0 – $S_1 O_0^0$ photoelectron band of indole–Ar shows a low-frequency progression due to a vdW bending mode whose frequency has been found to be 13 cm^{-1} . The assignments of low-frequency fundamental vibrational modes for the neutral indole have been reexamined by using the 6-311G** basis set.

1. Introduction

The indole heterocyclic ring system attracts considerable attention because of its role in protein spectroscopy due to the presence in the side chain of the amino acid tryptophan.¹ A considerable effort has been devoted to the interpretation of the indole ground state vibrational spectra.^{2–8} A room-temperature vapor-phase electronic spectrum and vibrational assignments of some fundamental frequencies in the S_1 state of indole have been published earlier by Hollas.⁹ A rotational analysis of the O_0^0 transition of indole has been carried out by Mani and Lombardi.¹⁰ Recently jet-cooled $S_1 \leftarrow S_0$ excitation spectra of indole have been reported by several authors.^{11–14} Bickel *et al.*¹⁵ and Nibu *et al.*¹⁶ have carried out a vibronic analysis of the S_1 state on the basis of dispersed laser-induced fluorescence (LIF) data. From a recent two-photon resonant four-photon ionization study, Cable¹⁷ has confirmed that the 1L_b state of indole is the first excited state. In a very recent study on rotationally resolved LIF spectra, Berden *et al.*¹⁸ have provided the orientation of the $^1L_b \leftarrow S_0$ transition moment.

A vibronic analysis of resonantly enhanced multiphoton ionization (REMPI) recently reported by Barstis *et al.*¹⁹ and the fluorescence studies have pointed out that there are no 1L_a transitions in indole in the range up to 1000 cm^{-1} above the 1L_b state origin. Sammeth *et al.*²⁰ have suggested from their two-photon polarized fluorescence spectra of indole that two bands located at 455 and 480 cm^{-1} above the 1L_b origin derive their intensities from the 1L_a state.

The van der Waals (vdW) complexes of indole attract attention as model species for the investigation of spectral properties of the tryptophanyl moiety within the protein environment. In a study of LIF and REMPI on vdW complexes of indole with polar molecules in supersonic jets, Tubergen and Levy²¹ have shown the sensitivity of the 1L_a – 1L_b gap to the solvent nature and larger S_1 origin red shifts exceeding 400

cm^{-1} . Vibrational predissociations for the indole– Ar_n ($n = 1, 2$) and indole– $(\text{CH}_4)_1$ vdW complexes have been studied by Outhouse *et al.*²² by dispersed LIF spectroscopy. According to a study of threshold-photoionization mass spectra, the adiabatic ionization energy (I_a) in indole– $(\text{CH}_4)_n$ ($n = 1, 2$) decreases approximately by 450 cm^{-1} per each coordinated methane molecule.²³ It has also been shown that I_a of indole– H_2O is lower by 3027 cm^{-1} than that of the bare indole.^{24,25}

The zero kinetic energy (ZEKE) photoelectron spectroscopy developed by Müller-Dethlefs, Schlag, and their co-workers^{26,27} has proved to be an efficient method for the investigation of cation vibrational states. Kimura and his co-workers have developed a compact high-brightness cm^{-1} -resolution ZEKE photoelectron analyzer that has a short flight distance,²⁸ and they have applied it extensively to carry out cation spectroscopy for various jet-cooled molecules and vdW complexes.^{29–36,38} The excitation step within the REMPI scheme allows us to carry out a state/species selective spectroscopy of products in the supersonic expansion. Two-color ZEKE photoelectron spectroscopy is capable of determining ionization energies with a high accuracy and allows the observation of low-frequency vibrational bands associated with weak vdW interactions. Condensed aromatic hydrocarbons and their vdW complexes are interesting subjects in ZEKE photoelectron studies from the viewpoints of vibronic interactions in their ground cationic state³⁴ and geometrical structures in their rare-gas vdW complexes.^{35,36}

The aim of the present ZEKE photoelectron study is (1) to determine accurate adiabatic ionization energies for indole and its vdW complex with Ar, (2) to identify various low-frequency fundamental vibrational modes in the cation ground state, and (3) to prove the vdW interaction of indole with Ar in the cationic state. In the present work, *ab initio* calculations of vibrational modes have also been carried out for indole in the ground state.

Indole is a planar molecule of C_s symmetry with 42 normal modes. Thirteen of them are out-of-plane (non-totally symmetric, a'') and 29 are in-plane (totally symmetric, a'). The numbering convention of Mulliken³⁷ is used throughout the text.

* To whom correspondence should be addressed. E-mail: k-kimura@jaist.ac.jp

[⊗] Abstract published in *Advance ACS Abstracts*, March 1, 1997.

2. Experimental Section

A detailed description of the experimental setup has been published elsewhere.^{35,38,39} Only a brief outline is given here. The supersonic free jet was produced by a pulsed valve (General Valve) with an orifice diameter of 0.8 mm. Argon was used as a carrier gas, and the stagnation pressure was in the range 3.5–4.0 atm. Indole (Nacalai Tesque, Extra Pure Grade) was used without further purification and seeded in argon at a temperature of approximately 100 °C. The valve was maintained at a temperature approximately 10 °C higher to prevent any condensation.

Two dye lasers (Quanta-Ray, PDL-3) were pumped by a nanosecond Nd:YAG laser (Quanta-Ray, GCR-190). The visible outputs (Rhodamine 590 for the first excitation and LDS 750 for the second excitation) were frequency doubled by KD*P crystals. The wavelengths of the dye lasers used were calibrated with a UV wavemeter (Burleigh Instruments, WA-5500). The counterpropagating laser beams intersected the pulsed jet at a right angle. ZEKE photoelectrons were collected by a two-pulsed-field ionization technique.³⁹ At approximately 50 ns after the laser shot a discrimination field (V_1) was applied, which removes the fast and near threshold electrons to reach the detector. After a variable delay (typically several hundreds of nanoseconds), a pulsed field with the opposite sign ($V_2 > -V_1$) was applied that ionizes the deeper Rydberg states and accelerates them toward the detector. The “depth” of the ionized states is given by the relation ΔE (cm^{-1}) = $(4-6) V^{1/2}$ ($V \text{ cm}^{-1}$). The typical voltages V_1 and V_2 were 0.7 and 1.3 $V \text{ cm}^{-1}$, respectively. The ionization energies were not corrected for the electric field shift, which can be estimated to be in the interval 4.6–6.8 cm^{-1} . A 20 cm long time-of-flight analyzer of a Wiley-McLaren design⁴⁰ was used for recording mass-selected REMPI ion-current spectra.

Ab initio quantum chemical calculations of vibrational frequencies for indole in the neutral ground state were carried out with the Gaussian-94 program package⁴¹ by using the 6-311G** basis set. A full geometry optimization was carried out within the C_s symmetry.

3. Results and Discussion

3.1. REMPI Mass-Selected Ion-Current Spectra. The one-color (1 + 1) REMPI spectrum of indole in the range 35 200–36 040 cm^{-1} is presented in Figure 1. The S_1 origin found at 35 235 $\pm 1 \text{ cm}^{-1}$ agrees with the previously reported values.^{12,13,16} The vibronic levels are summarized in Table 1, together with the vibrational assignments based on the dispersed fluorescence data of Bickel *et al.*¹⁵ and Nibu *et al.*¹⁶ An additional weak band at 694 cm^{-1} may be identified and tentatively assigned to the 29¹42² combination. The S_1 origin of the indole-Ar vdW complex is red-shifted by 27 cm^{-1} , close to a value of 26 cm^{-1} reported by Outhouse *et al.*²² The transition does not exhibit any low-frequency features attributable to the vdW vibrational mode (see the inset in Figure 1).

3.2. ZEKE Photoelectron Spectra of Indole. The (1 + 1') ZEKE photoelectron spectra of bare indole, obtained via eight S_1 vibrational levels, namely, 0⁰, 42², 41², 29¹, 28¹, 27¹, 26¹, and 37², are shown in Figures 2 and 3. The excess energies of the bands above the cation vibrationless D_0 state are summarized in Table 2. The band appearing in the spectrum in Figure 2a, obtained via the vibrationless S_1 state at 27 357 cm^{-1} , may be attributed to the cation vibrationless D_0 state. The adiabatic ionization energy (I_a) derived from this peak amounts to 62 592 $\pm 4 \text{ cm}^{-1}$ (7.7604 \pm 0.0005 eV). Hager *et al.*^{24,25} have obtained an I_a value of 62 598 cm^{-1} from their two-color photoionization mass spectra.

TABLE 1: Vibrational Assignments of Indole in the S_1 State, Deduced from the REMPI Ion-Current Spectrum

energy (cm^{-1})	displacement from S_1 0 ⁰ (cm^{-1})	intensity ^a	vibrational assignment
35 235	0	100	0 ⁰
35 253	18	4	sequence
35 551	316	8	42 ²
35 600	365	12	41 ²
35 615	380	16	29 ¹
35 671	436	3	39 ¹ 42 ¹
35 690	455	18	39 ¹ 41 ¹
35 715	480	33	28 ¹
35 749	514	1	40 ²
35 759	524	2	37 ¹ 42 ¹
35 774	539	22	27 ¹
35 784	558	4	39 ²
35 823	588	2	
35 929	694	3	29 ¹ 42 ²
35 952	717	65	26 ¹
35 971	736	36	37 ²
36 007	772	4	36 ¹ 39 ¹ /40 ¹ 41 ² 42 ¹
36 017	782	14	29 ¹ 40 ¹ 42 ¹ /39 ¹ 40 ¹ 42 ¹

^a Values are not corrected for the laser intensity variations.

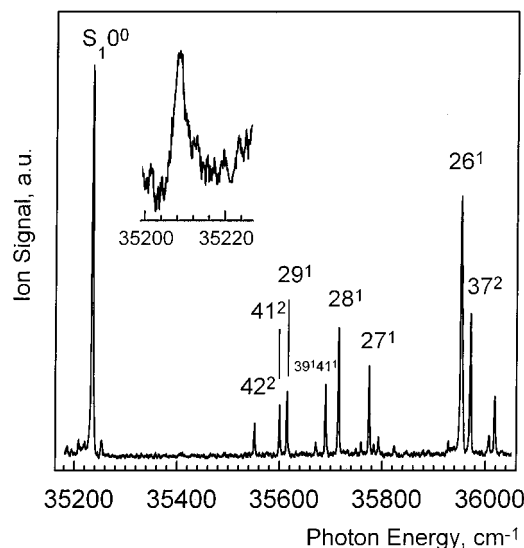


Figure 1. One-color (1+1) REMPI mass-selected ion-current spectra of indole and the indole-Ar vdW complex. The inset shows the S_1 origin (O_0^0) band of indole-Ar. The red shift in the S_1 origin for indole-Ar amounts to 27 cm^{-1} with respect to indole. The assignments for weak peaks are given in Table 1.

The highest intensity of the vertical transition via the vibrationless S_1 state (Figure 2) clearly indicates no major change of geometry upon ionization. The $\Delta v = 0$ propensity can thus provide an efficient clue to the assignments of the ZEKE features. Any non-totally symmetric vibrational levels are absent from the S_1 - S_0 REMPI spectrum (Figure 1), and only two-quantum transitions are observable for the 42 and 41 out-of-plane modes, in accordance with the symmetry consideration. The ZEKE spectrum obtained via the totally symmetric S_1 vibrationless state (Figure 2a) shows two low-frequency vibrational transitions with intervals of 193 and 233 cm^{-1} (see Table 2a). Assuming the $\Delta v = 0$ propensity, the photoelectron spectra obtained via the S_1 42² and 41² levels provide values of 385 and 468 cm^{-1} for the two vibrational quanta, respectively (Figure 2a,b). Thus the first two peaks above the D_0 origin in the ZEKE spectrum obtained via the S_1 origin may be assigned to the D_0 42¹ and 41¹ levels. The 42 and 41 vibrational progressions are observable up to $v = 3$. Any assignments to the excitation of two vibrational quanta would imply that $\Delta v = 2$ vertical transitions take place via S_1 42² and 41², which

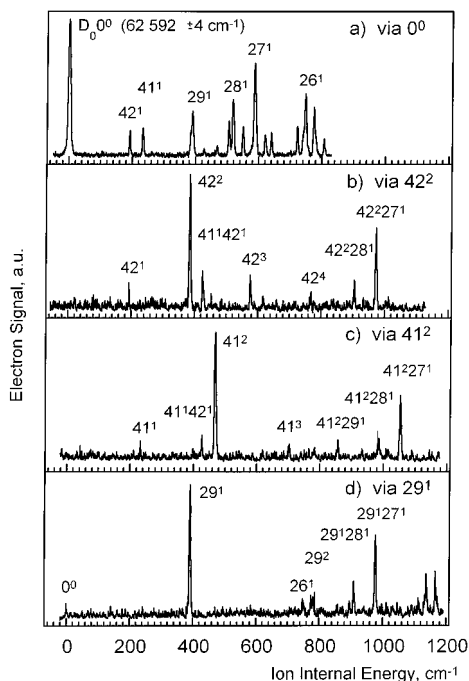


Figure 2. Two-color (1+1') ZEKE photoelectron spectra of indole, obtained via the following vibrational levels of the S_1 state: (a) 0^0 , (b) 42^2 , (c) 41^2 , and (d) 29^1 . Only the dominant peaks are labeled. For the assignments of other vibrational bands, see Table 2.

are rather improbable for out-of-plane vibrational modes. Clearly the one-quantum transitions of the non-totally symmetric modes indicate the presence of the vibronic interactions in the ground cation state.

The D_0 state is formed by the removal of a π electron. Thus the D_0 vibronic levels of the non-totally symmetric mode are a' for $\nu = \text{odd}$ and a'' for $\nu = \text{even}$. The a' vibronic levels may gain their intensities from the coupling with a cation state formed by a σ electron removal. The vibrational progressions are observed up to $\nu = 3$ and 4, when the S_1 42^2 and 41^2 levels are pumped, respectively. The ZEKE spectra obtained via the totally symmetric levels S_1 29^1 (Figure 2d) and 28^1 , 27^1 , and 26^1 (Figure 3a–c) provide straightforward assignments for the peaks observed at 390, 518, 587, and 748 cm^{-1} to these levels. The ZEKE spectrum obtained via the S_1 origin shows further bands at 505, 550, 640, and 807 cm^{-1} (see Table 2a). These bands seem not to be due to any combination levels.

The frequency of the 39 mode has been derived to be 385 cm^{-1} from the ZEKE spectrum obtained via the S_1 39^142^1 level (Table 2e). The spectrum obtained via the S_1 37^2 level (Figure 3d) exhibits three strong bands around 1000 cm^{-1} above the D_0 origin. The most intensive transition yields a frequency of 529 cm^{-1} for the 37 mode. This assignment is supported by the appearance of a band at 722 cm^{-1} (Figure 2a), which may come from the combination level 37^142^1 . The bands at 997 and 1017 cm^{-1} may gain some of their intensities from the 25^142^1 and 36^141^2 combinations, but some higher vibrational modes can also contribute to the high intensities of these bands.

Given the frequencies of the 37 and 39 modes, the band observed at 505 cm^{-1} may be tentatively assigned to the 38 out-of-plane mode. Consequently the peaks at 550 and 640 cm^{-1} may come from the 36 and 35 out-of-plane modes, respectively, since all the low-frequency in-plane modes up to 750 cm^{-1} are identified. The remaining 755 and 807 cm^{-1} bands in the spectrum obtained via the S_1 origin may be tentatively assigned on the basis of the neutral ground state frequencies. The vibrational frequencies in the cation D_0 state

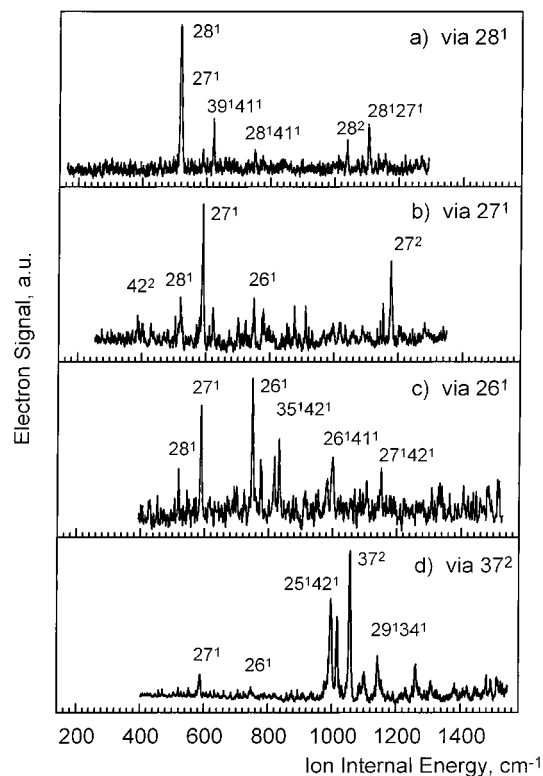


Figure 3. Two-color (1+1') ZEKE photoelectron spectra of indole, obtained via the following vibrational levels of the S_1 state: (a) 28^1 , (b) 27^1 , (c) 26^1 , and (d) 37^2 . Only the dominant peaks are labeled. For the assignments of other vibrational bands, see Table 2.

are generally lower than in the S_0 state. The 807 cm^{-1} peak thus may be due to the excitation to the 25^1 level rather than to the 34^1 level. The out-of-plane 33 mode might be assigned to this peak. However, the former assignment is preferred because of the generally larger Franck–Condon factors observed for the in-plane modes.

The observed vibrational structure in the ZEKE spectra is consistent with the absence of any significant contribution of the 1L_a state origin to the intermediate levels. If there is any significant contribution from the higher 1L_a origin to the intermediate levels studied, any ZEKE vibrational structure similar to that found for the $S_1(^1L_b)$ origin is expected to appear.

The vibrational frequencies and their assignments in the S_0 , S_1 , and D_0 states of indole are summarized in Table 3, together with the results of the present S_0 normal coordinate analysis based on the 6-311G** calculations. Generally the vibrational frequencies in the D_0 state fall between the S_0 and S_1 states. There is a controversy in the assignment of the 488 cm^{-1} band in the S_0 state. Collier⁶ has assigned this feature to overtone and combination frequencies on the basis of AM1 semiempirical calculations. According to the normal coordinate analysis of Takeuchi and Harada,⁵ this band is due to the 38 mode. Barstis *et al.*¹⁹ have supported this interpretation by their 3-21G calculations. However, to deduce a reasonable agreement with the experimental frequencies, two significantly different scaling factors should be used for the in-plane and out-of-plane modes.

The fundamental frequencies obtained from the present 6-311G** basis set are shown in Table 3, in excellent agreement with the experimental values. A single scaling factor has been found to be sufficient for the in-plane and out-of-plane modes except for the 488 cm^{-1} vibration. Also the change in the frequency of the 38 mode upon ionization is more consistent with the other modes in the present assignments. Figure 4 shows

TABLE 2: Vibrational Assignments of the Indole Cation in the Ground State (D_0), Deduced from the ZEKE Photoelectron Spectra

ion internal energy (cm^{-1})			ion internal energy (cm^{-1})		
relative intensity ^a	vibrational assignment	relative intensity ^a	vibrational assignment	relative intensity ^a	vibrational assignment
(a) via S_1 O^0					
0	100	0^0	587	67	27^1
192	18	42^1	620	14	$39^1 41^1 / 41^1 42^2$
233	20	41^1	640	17	35^{1b}
385	sh	42^2	701	3	41^3
390	31	29^1	722	21	$37^1 42^1$
426	4	$41^1 42^1$	742	sh	$36^1 42^{1b}$
468	7	41^2	748	45	$26^1 / 28^1 41^1$
505	21	38^{1b}	755	sh	34^{1b}
518	40	28^1	774	35	$29^1 42^2 / 29^1 39^1$
550	21	36^{1b}	781	sh	29^2
578	sh	42^3	807	11	25^{1b}
(b) via S_1 42^2					
193	14	42^1	617	15	$41^1 42^2$
385	100	42^2	767	11	42^4
426	28	$41^1 42^1$	905	20	$28^1 42^2$
576	9	42^3	973	61	$27^1 42^2$
(c) via S_1 41^2					
232	14	41^1	857	16	$29^1 41^2$
426	18	$41^1 42^1$	985	18	$28^1 41^2$
468	100	41^2	1052	51	$27^1 41^2$
703	8	41^3			
(d) via S_1 29^1					
0	9	0^0	909	25	$28^1 29^1$
391	100	29^1	977	60	$27^1 29^1$
749	27	$26^1 / 28^1 41^1$	1112	11	$29^1 37^1 42^1$
775	14	$29^1 39^1 / 29^1 42^2$	1137	30	$26^1 29^1$
781	15	29^2	1165	32	$29^2 42^2 / 29^2 39^1$
857	8	$29^1 41^2$	1171	sh	29^3
896	10	$29^1 38^{1b}$			
(e) via S_1 $39^1 42^1$					
577	100	$39^1 42^1$			
(f) via S_1 28^1					
518	100	28^1	750	14	$28^1 41^1 / 26^1$
588	14	27^1	1039	21	28^2
621	38	$39^1 41^1 / 41^1 42^2$	1105	31	$27^1 28^1$
(g) via S_1 27^1					
387	19	42^2	873	28	$35^1 41^{1b}$
520	33	28^1	908	29	$28^1 42^2$
587	100	27^1	992	15	$25^1 42^{1b}$
619	27	$39^1 41^1 / 41^1 42^2$	1015	16	$36^1 41^{2b}$
697	19	$38^1 42^{1b}$	1032	13	$37^1 38^1$
721	17	$37^1 42^1$	1150	30	$27^1 41^2$
746	35	26^1	1174	58	27^2
775	27	$29^1 42^1 / 29^1 39^1$			
(h) via S_1 26^1					
519	38	28^1	832	57	$35^1 42^{1b}$
588	86	27^1	981	24	$26^1 41^1$
748	100	26^1	1000	43	$25^1 42^{1b}$
776	41	$29^1 42^2 / 29^1 39^1$	1106	24	$27^1 28^1$
818	43	$29^1 41^1 42^1$	1151	32	$27^1 41^2$
(i) via S_1 37^2					
588	13	27^1	1086	9	$25^1 42^2$
747	6	26^1	1100	17	36^{2b}
997	65	$25^1 42^{1b}$	1144	27	$29^1 34^{1b}$
1017	52	$36^1 41^{2b}$	1261	22	
1057	100	37^2	1308	11	

^a Relative intensities are not corrected for the variation in laser intensity. ^b Tentative assignment, not supported by the $\Delta\nu = 0$ propensity for the particular fundamental mode.

the plots of the experimental values against the calculated ones for both the vibrational assignments. The 40 mode deviates from the fit. A closer inspection of this mode reveals a large amplitude of the N-H bending. The anharmonicity of the

TABLE 3: Vibrational Frequencies of Indole (in cm^{-1}) in the S_1 and D_0 States, Observed in the REMPI and ZEKE Spectra, Respectively; *ab Initio* and Experimental Frequencies in the S_0 State Are Also Shown for Comparison

mode	S_0		S_1 exptl	D_0 exptl
	exptl ^a	calc ^c		
Non-Totally Symmetric Modes				
42	225	211	158	193
41	256	243	183	233
40	403	340	257	
39	426	433	279	385
38	586	580	316 ^d	505 ^b
37	607	612	368	529
36	722	744	493	550 ^b
35	748	767		640 ^b
34	780	792		755 ^b
33	853	878		
Totally Symmetric Modes				
29	398	396	380	391
28	543	539	480	518
27	608	608	539	587
26	763	754	717	748
25	873	868		807 ^b

^a Experimental values in the S_1 state (ref 5). ^b Tentative assignment, not supported by any ZEKE photoelectron measurements via this particular S_1 intermediate level. ^c Calculated values scaled down by a factor of 0.92. ^d Derived from the assignment of the combination bands (ref 19).

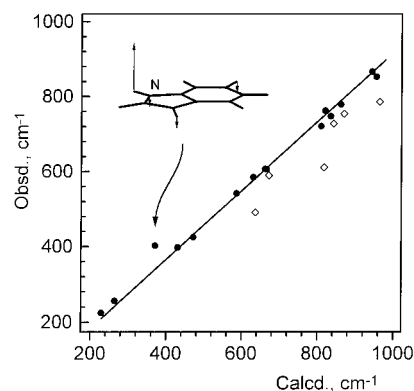


Figure 4. Plots of the observed vibrational frequencies against the calculated ones in the S_0 state of indole. Filled circles represent the assignments of Collier (ref 6). Empty diamonds show the assignments of Takeuchi and Harada (ref 5). The inset shows the vibration of the 40 mode.

bending potential may be responsible for the deviation from the calculated value.

3.3. ZEKE Photoelectron Spectrum of Indole-Ar. The $(1 + 1')$ ZEKE spectrum of the indole-Ar vdW complex obtained via the S_1 origin is presented in Figure 5. The adiabatic ionization energy of indole-Ar has been found to be $I_a = 62\,504 \pm 6 \text{ cm}^{-1}$. The decrease in I_a upon the complex formation amounts to be 88 cm^{-1} . The S_1 energies and the I_a values are summarized in Table 4.

The decrease in I_a upon complex formation for the benzene-Ar vdW complex is reported to be 172 cm^{-1} ,⁴² whereas those for naphthalene-Ar³⁶ and anthracene-Ar³⁵ are significantly smaller, namely, 85 and 65 cm^{-1} , respectively. In the vdW complexes of substituted benzenes with Ar,^{43,44} an electron-accepting group strongly stabilizes the cation complexes, whereas an electron-donating group brings about a destabilization relative to the unsubstituted aromatics. The decrease in I_a for the aniline-Ar complex amounts to 111 cm^{-1} .⁴⁴ Therefore, the I_a decrease of 88 cm^{-1} found for indole-Ar in the present

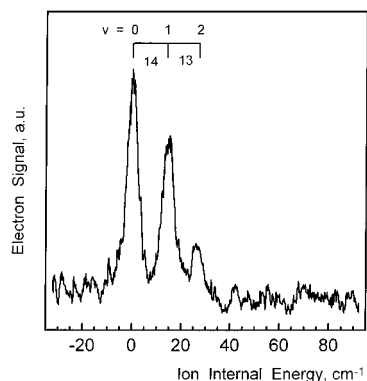


Figure 5. Two-color (1+1') ZEKE photoelectron spectrum of the indole-Ar vdW complex, obtained via the S_1 origin.

TABLE 4: Summary of the S_1 Origins (S_1 0^0) and the Adiabatic Ionization Energies (I_a) for Indole and Its vdW Complex with Ar (in cm^{-1}); Shifts in the Energies upon the Complex Formation Are Also Shown

	S_1 0^0 (cm^{-1})	ΔS_1 0^0 (cm^{-1})	I_a (cm^{-1})	ΔI_a (cm^{-1})
indole	35 235		62 592	
indole-Ar	35 208	-27	62 504	-88

work agrees with the trend found for the condensed aromatic hydrocarbons as well as for the electron donor/accepting character of the heteroatom.

The ZEKE spectrum of indole-Ar (Figure 5) exhibits a 13–14 cm^{-1} progression, which is missing in that of bare indole. It is reported that the frequencies associated with the vdW stretching vibration between an aromatic hydrocarbon and a rare-gas atom are in the range 40–50 cm^{-1} and those of the bending modes are in the range 10–16 cm^{-1} .^{45–50} The vibrational structure in Figure 5 may be assigned to a vdW bending mode in the indole-Ar cation. From the narrow $\Delta v = 0$ Franck-Condon envelope as well as from the spectral feature observable only up to $v = 2$, it is indicated that there is only a slight change in the geometry of the complex upon ionization.

The charge-induced dipole interaction mainly contributes to the I_a decrease.⁵¹ The value of $\Delta I_a = 88 \text{ cm}^{-1}$ in indole-Ar is nearly identical to that of naphthalene-Ar, indicating that the argon atom sees a similar charge distribution. In naphthalene-Ar, the argon atom resides above the point of symmetry of naphthalene.³⁶ An analogous geometry may be assumed for indole-Ar.

4. Conclusions

In the present work on indole and its vdW complex with Ar under jet-cooled conditions, using two-color (1+1') ZEKE photoelectron spectroscopy, we have been able to determine their adiabatic ionization energies (I_a) very accurately as well as to observe various cation low-frequency vibrational modes in the region approximately 800 cm^{-1} above the D_0 origin. The following conclusions have been deduced. (1) The ZEKE spectra are consistent with the absence of the 1L_a transitions in the region within 800 cm^{-1} above the $S_1(^1L_b)$ origin. (2) The geometry of indole does not undergo any significant geometry change upon ionization. (3) The non-totally symmetric vibrational levels are populated in the cation D_0 state because of a significant vibronic interaction in the D_0 state. (4) The ionization energy decrease of indole-Ar falls within the values reported for condensed aromatics, suggesting that the argon atom is located above the "center" of the aromatic moiety. (5) Only a minor change of the position of the argon atom occurs upon ionization in indole-Ar.

The two-color REMPI-ZEKE photoelectron spectroscopy has proved to be an efficient tool for providing accurate adiabatic ionization energies of jet-cooled molecules and vdW complexes as well as for elucidating their cation low-frequency vibrational modes including vdW vibrations.

Acknowledgment. T.V. wishes to express his thanks to the Japan Society for the Promotion of Science for the financial support under the Foreign Researchers Invitation Program during the period of this research.

References and Notes

- (1) Creed, D. *Photochem. Photobiol.* **1984**, *39*, 537.
- (2) Lautie, A.; Lautie, M. F.; Gruger, A.; Fakhri, S. A. *Spectrochim. Acta* **1980**, *36A*, 85.
- (3) Hirakawa, A. Y.; Nishimura, Y.; Matsumoto, T.; Nakanishi, M.; Tsuboi, M. *J. Raman Spectrosc.* **1978**, *7*, 282.
- (4) Smithson, T. L.; Shaw, R. A.; Wieser, H. *J. Chem. Phys.* **1984**, *81*, 4281.
- (5) Takeuchi, H.; Harada, I. *Spectrochim. Acta* **1986**, *42A*, 1069.
- (6) Collier, W. *J. Chem. Phys.* **1988**, *88*, 7295.
- (7) Suwaiyan, A.; Zwarich, R. *Spectrochim. Acta* **1986**, *42A*, 1017.
- (8) Majoube, M.; Vergoten, G. J. *J. Raman Spectrosc.* **1992**, *23*, 431.
- (9) Hollas, J. M. *Spectrochim. Acta* **1963**, *19*, 755.
- (10) Mani, A.; Lombardi, J. R. *J. Mol. Spectrosc.* **1969**, *31*, 308.
- (11) Hager, J. W.; Wallace, S. C. *J. Phys. Chem.* **1983**, *87*, 2121.
- (12) Hager, J. W.; Demmer, D. R.; Wallace, S. C. *J. Phys. Chem.* **1987**, *91*, 1375.
- (13) Bersohn, R.; Even, U.; Jortner, J. *J. Chem. Phys.* **1984**, *80*, 1050.
- (14) Phillips, L. A.; Levy, D. H. *J. Chem. Phys.* **1986**, *85*, 1327.
- (15) Bickel, G. A.; Demmer, D. R.; Outhouse, E. A.; Wallace, S. C. *J. Chem. Phys.* **1989**, *91*, 6013.
- (16) Nibu, Y.; Abe, H.; Mikami, N.; Ito, M. *J. Phys. Chem.* **1983**, *87*, 3898.
- (17) Cable, J. R. *J. Chem. Phys.* **1990**, *92*, 1627.
- (18) Berden, G.; Meerts, W. L.; Jalviste, E. *J. Chem. Phys.* **1995**, *103*, 9596.
- (19) Barstis, T. L. O.; Grace, L. I.; Dunn, T. M.; Lubman, D. M. *J. Phys. Chem.* **1993**, *97*, 5820.
- (20) Sammeth, D. M.; Yan, S.; Spangler, L. H.; Callis, P. R. *J. Phys. Chem.* **1990**, *94*, 7340.
- (21) Tubergen, M. J.; Levy, D. H. *J. Phys. Chem.* **1991**, *95*, 2175.
- (22) Outhouse, E. A.; Bickel, G. A.; Demmer, D. R.; Wallace, S. C. *J. Chem. Phys.* **1991**, *95*, 6261.
- (23) Hager, J. W.; Wallace, S. C. *Oxford Ser. Opt. Sci.* **1990**, *1* (Lasers and Mass Spectrometry), 423.
- (24) Hager, J. W.; Ivanco, M.; Smith, M. A.; Wallace, S. C. *Chem. Phys. Lett.* **1985**, *113*, 503.
- (25) Hager, J. W.; Ivanco, M.; Smith, M. A.; Wallace, S. C. *Chem. Phys.* **1986**, *105*, 397.
- (26) Müller-Dethlefs, K.; Sander, M.; Schlag, E. W. *Z. Naturforsch. A* **1984**, *39*, 1089.
- (27) Müller-Dethlefs, K.; Sander, M.; Schlag, E. W. *Chem. Phys. Lett.* **1984**, *112*, 291.
- (28) Takahashi, M.; Ozeki, H.; Kimura, K. *Chem. Phys. Lett.* **1991**, *181*, 255.
- (29) Cockett, M. C. R.; Takahashi, M.; Okuyama, K.; Kimura, K. *Chem. Phys. Lett.* **1991**, *187*, 250.
- (30) Kimura, K.; Takahashi, M. *Optical Methods for Time- and State-Resolved Chemistry*; Ng, C. Y., Ed.; SPIE-The International Society for Optical Engineering: Bellingham, WA, 1992; Vol. 1638, p 216.
- (31) Ozeki, H.; Takahashi, M.; Okuyama, K.; Kimura, K. *J. Chem. Phys.* **1991**, *95*, 9401.
- (32) Okuyama, K.; Cockett, M. C. R.; Kimura, K. *J. Chem. Phys.* **1992**, *97*, 1649.
- (33) Takahashi, M.; Kimura, K. *J. Chem. Phys.* **1992**, *97*, 2920.
- (34) Cockett, M. C. R.; Ozeki, H.; Okuyama, K.; Kimura, K. *J. Chem. Phys.* **1993**, *98*, 1763.
- (35) Cockett, M. C. R.; Kimura, K. *J. Chem. Phys.* **1994**, *100*, 3429.
- (36) Vondrák, T.; Sato, S.; Kimura, K. *Chem. Phys. Lett.* **1996**, *261*, 481.
- (37) Mulliken, R. S. *J. Chem. Phys.* **1955**, *23*, 1997.
- (38) Takahashi, M.; Ozeki, H.; Kimura, K. *Chem. Phys. Lett.* **1991**, *181*, 255.
- (39) Sato, S.; Kimura, K. *Chem. Phys. Lett.* **1996**, *249*, 155.
- (40) Wiley, W. C.; McLaren, I. H. *Rev. Sci. Instrum.* **1955**, *26*, 1150.
- (41) Frisch, M. J.; Trucks, G. W.; Schlegel, H. B.; Gill, P. M. W.; Johnson, B. G.; Robb, M. A.; Cheeseman, J. R.; Keith, T. A.; Petersson, G. A.; Montgomery, J. A.; Raghavachari, K.; Al-Laham, M. A.; Zakrzewski, V. G.; Ortiz, J. V.; Foresman, J. B.; Cioslowski, J.; Stefanow, B. B.; Nanayakkara, A.; Challacombe, M.; Peng, C. Y.; Ayala, P. Y.; Chen, W.;

Wong, M. W.; Andres, J. L.; Replogle, E. S.; Gomperts, R.; Martin, R. L.; Fox, D. J.; Binkley, J. S.; Defrees, D. J.; Baker, J.; Stewart, J. P.; Head-Gordon, M.; Gonzales, C.; Pople, J. A. *Gaussian 94* (Revision C.3); Gaussian Inc.: Pittsburgh, PA, 1995.

(42) Chewter, A.; Müller-Dethlefs, K.; Schlag, E. W. *Chem. Phys. Lett.* **1987**, 135, 219.

(43) Araki, M.; Sato, S.; Kimura, K. *J. Phys. Chem.* **1996**, 100, 10542.

(44) Takahashi, M.; Ozeki, H.; Kimura, K. *J. Chem. Phys.* **1992**, 96, 6399.

(45) Ramaekers, J. J. F.; van Dijk, H. K.; Langelaar, J.; Rettschnick, R. P. H. *Faraday Discuss. Chem. Soc.* **1983**, 75, 183.

(46) Brumbaugh, D. V.; Kenny, J. E.; Levy, D. H. *J. Chem. Phys.* **1983**, 78, 3415.

(47) Menapace, J. A.; Bernstein, E. R. *J. Phys. Chem.* **1987**, 91, 2533.

(48) Jacobson, B. A.; Humphrey, S.; Rice, S. A. *J. Chem. Phys.* **1988**, 78, 5624.

(49) Weber, P. M.; Buontempo, J. T.; Novak, F.; Rice, S. A. *J. Chem. Phys.* **1988**, 88, 6082.

(50) Weber, P. M.; Rice, S. A. *J. Chem. Phys.* **1988**, 88, 6107.

(51) Bieske, E. J.; Rainbird, M. W.; Atkinson, I. M.; Knight, A. E. W. *J. Chem. Phys.* **1989**, 91, 752.